IoT-Based Diabetic Retinopathy Detection Using a Novel KL-CNN

Mohammed Hameed Alhameed*

College of Computer Science and Information Technology, Jazan University, Jazan 82817, Kingdom of Saudi Arabia

Corresponding author; malhameed@jazanu.edu.sa

Abstract: *One of the main causes of avertible blindness is Diabetic Retinopathy (DR). Thus, patients could be prevented from visual loss by DR's early detection. Various detection techniques are present. However, they do not provide better outcomes owing to the presence of minute parts of vessels and exudates. Thus, this work proposes a novel Kriging Layer-centric Convolution Neural Network (KL-CNN)-based retinopathy detection method. Primarily, preprocessing is done. After that, by utilizing Linear Interpolation-centered Contrast Limited Adaptive Histogram Equalization (LI-CLAHE), the image's contrast is enhanced. The RESNIK-based Watershed Segmentation Algorithm (RWSA) is performed for segmenting the blood vessels from the enhanced image. The features are extracted from the segmented blood vessels. Lastly, the obtained features and the attributes, which are presented in the corresponding diabetic dataset, are directly given into the KL-CNN to classify its complexities into normal, mild, moderate, severe, along with proliferate. The proposed system's experiential outcomes are analogized with the prevailing approaches, which exhibit higher efficacy as well as accuracy with 98.4%. In addition, a specificity of 96.4%, a precision of 96.7%, a recall of 96.23%, and an f-measure of 91.7% are obtained*

Keywords: Diabetic retinopathy (DR), fundus Image, Deep learning, medical informatics, Retinal image, Internet of Things (IoT).

1. INTRODUCTION

"Health" is primary for all human beings (Rajkumar R.S. et al., 2021). Currently, the majority of the population suffers from Diabetes Mellitus (DM), which is prevailing globally. The name of the chronic disease is DM, which is generally named diabetes. It is caused owing to higher glucose levels in the person's blood affected by it (Chaudhary & Ramya, 2020). Each eye along with the nerve system as well as the kidneys, heart, and different organs are affected by this damage. A rare disease caused by higher blood sugar levels is named DR (Habib Raj et al., 2020). It causes blindness to many people worldwide and the majority of them do not have any symptoms until the last stage. Early detection, which could enable timely treatment for slowing down the disease's progression, is the only measure for maintaining better eyesight and preventing blindness (Sabbir et al., 2020). Macula, optic discs, and blood vessels are the healthy retina's major components. Also, any disparities in these components are the eye disease's symptoms. DR is broadly classified as proliferate and non-proliferate. By blood leakage along with fluid on the retinal surface, non-proliferative occurs. The excess formation of blood vessels in the retina image is indicated by the proliferative (Qiao et al., 2020).

Hemorrhages, cotton woolen spots, microaneurysms, and exudates are the non-proliferative DR's pathological signs. The complexities of DR will be identified grounded on these signs. Microaneurysms, which are tiny aneurysms or swellings in the blood vessel's wall, are the initial pathological symptom (Maneerat et al., 2020). Exudates are leaking of proteins as well as lipids as of the bloodstream into the retina via damaged blood vessels. Hard exudate formation seems yellowish with various shapes along with

sizes. By gathering the features as of the fundus input image, the DR detection is executed. By utilizing an Internet of Things (IoT) device, the images are scanned and collected from the patient. The IoT device gives an image with the specifications of different colors, degrees, et cetera. However, an ophthalmologist is required in the DR diagnosis utilizing fundus images for diagnosing the DR's minute features. Also, this process is time-consuming (Jayakumari et al., 2020). Thus, there is a demand for developing reliable auto-DR screening techniques (Li et al., 2021). Utilizing various machine learning systems like Recurrent Neural Network (RNN), Artificial Neural Network (ANN), Convolution Neural Network (CNN), Deep Neural Network (DNN), et cetera, the automatic detection technique is modeled to test for DR (Kolla & Venugopal, 2021). Generally, a vital requirement in the medical area is the Machine learning system. By classifying the disease complications, the healthcare professional requires beneficial tools to diagnose medical illness. However, since there is no better concentration on the minute vessels, the modeled approaches are still daunting to provide better classification accuracy (Trisha & Ali, 2020).

Regardless of developing several ML and Deep Learning (DL)-centric models for DR detection, still, certain limitations are required to be resolved. For segmentation, one of the major challenges is the formation of neovascularization since it is structured with the minute. The images of low entropy had lower contrast levels. Conversely, higher entropy stands for a higher contrast level betwixt neighboring pixels. However, detecting proliferative grounded on entropy values is difficult since the proliferative vessels are greatly different from normal vessels. The complexity classification is done with more referral images by computing the threshold value in the existing ones. But, the iteration of the thresholding value is higher.

To surpass these issues, an enhanced DR detection system utilizing a novel KL-CNN classifier is proposed in this work. It comprises several research objectives, which are explained in this section. By considering the fundus image as the input, the proposed system is executed. A dark appearance was present in the fundus image. Hence, the information collected as of the image is challenging. Thus, primarily, by utilizing the novel Image Enhancement systems, the structure and clarity of an image are enhanced. The minute vessels are pondered in depth with the best segmentation model for the proper segmentation of blood vessels. By utilizing the novel Neural Network Classifier for classifying the complexities as normal, mild, moderate, severe, and proliferate, a higher detection rate and lower computation complexity are attained.
This paper's remaining part is organized as: Section 2 explicates the prevailing works. Section 3 elucidates the proposed framework. Section 4 illustrates the proposed technique's results and discussion grounded on performance metrics. Lastly, section 5 offers conclusions.

2. LITERATURE SURVEY

Huge amount of contribution made by various authors are as follows: (Albahli et al., 2021) established a custom faster region with a CNN model for the DR lesions' classification. For model training, the dataset annotations were engendered after pre-processing. For computing the key points' representative set, DenseNet-65 was introduced. Consequently, the input sample was localized and classified by Faster-RCNN into five classes. The experiential outcome demonstrated the developed model's robustness. However, the system had complex architecture.

(Tymchenko et al., 2020) explored an automatic DL-centric system for DR's stage detection. The multistage methodology was wielded to transfer learning. For the final solution, an ensemble of 3 CNN frameworks as well as transfer learning has been employed. The outcomes displayed that higher as well as stable outcomes were attained by the presented model. However, the system considered only some important features, which resulted in less accuracy.

(Chen et al., 2020) proffered a framework for retinal image classification regarding the multi-scale shallow CNNs' integration. To clean the noise existence, the input image was preprocessed. The image

classification was executed well while there were inadequate high-quality labeled samples due to feature sensing by diverse base learners as well as repeatable dataset sampling. The findings exposed that the enhanced model outperformed the prevailing model. However, the system could not be spatially invariant to the input data.

(Pao et al., 2020) propounded the entropy image computed by utilizing the fundus photograph's green component. Before computing the entropy images, pre-processing was done by utilizing Unsharp Masking (UM). The bi-channel CNN having inputs of both the entropy images were preprocessed by UM. Moreover, it advanced the referable DR's detection. The outcomes exhibited the model's better accuracy and sensitivity. However, owing to the UM, the edges of the images may miss.

(Gadekallu, Khare, Bhattacharya, Singh, Maddikunta, Ra, et al., 2020) established a DR's early detection utilizing the Principal Component Analysis (PCA). For extracting the features from the dataset, PCA was employed. For dimensionality reduction, the firefly algorithm was implemented. For classification, this diminished dataset was subjected to a Deep Neural Network Model. The results displayed the developed approach's superiority. Owing to the feature reduction technique, the spatial information disappeared.

(Mateen et al., 2020) suggested a pre-trained CNN-based framework for the exudates detection. For localizing the exudates' features, Region Of Interest (ROI) localization was wielded. By utilizing pre-trained CNN methodologies (Inception-v3, Residual Network-50, along with Visual Geometry Group Network-19), transfer learning was executed for feature extraction. Further, for exudate classification, the fused features as of FC layers were subjected to the softmax classifier. The outcomes illustrated that the developed technique was superior to the prevailing mechanisms. But, the training time of the developed model was high. (Samanta et al., 2020) elucidated the DR's automatic detection utilizing CNN on a small dataset. For enhancing the small regions of relevance in the image, CLAHE was applied. Hence, the experiential outcomes provided a better kappa score for the developed model. However, the prediction accuracy may get disturbed owing to the uneven Gray Level (GL).

(Bibi et al., 2020) propounded a computationally simple DR detection technique. Primarily, a segmentation independent '2' stage preprocessing-centered model was engendered that could efficiently retrieve DR pathognomonic signs. After that, as a feature descriptor for fundus images, the performance of Local Binary Patterns (LBP), Local Ternary Patterns (LTP), Dense Scale-Invariant Feature Transform (DSIFT), and Histogram of Oriented Gradients (HOG) was analyzed thoroughly. For the DR classification, Support Vector Machine (SVM) kernel-centric classifiers were employed. The outcomes exhibited that the presented model was very well-fitted and generalized than the prevailing model. However, it did not execute very well since the image has more noise.

(Math & Fatima, 2021) presented an Adaptive ML classification for DR. For getting the segment-level DR estimation, the pre-trained CNN was adopted. Finally, to deal with the irregular lesions of DR, an end-to-end segment-centered learning approach was employed. The results displayed that the developed technique had superior performance. But, the maintenance cost of the developed model was higher. (Gadekallu, Khare, Bhattacharya, Singh, Maddikunta, & Srivastava, 2020) exhibited a DNN for predicting DR. The DR dataset's standardization employing a standard scaler normalization model, ensued by dimensionality decline utilizing Principal Component Analysis (PCA). Then, selection of optimal hyperparameters by Grey Wolf Optimization (GWO), and finally dataset's training utilizing a DNN model were the steps involved here. The outcomes exposed that the developed system offered superior performance. However, the system was easily suspected of overfitting problems since it processes more features at a time.

3. PROPOSED METHODOLOGY FOR DETECTION OF DIABETIC RETINOPATHY

A novel KL-CNN Classifier for the efficient identification and detection of retinopathy is proposed in this manuscript. Two phases of input are considered for the patient, that is, the patient's fundus image and the corresponding patient's diabetes data. Blood vessels are segmented from the image. Then, the features are extracted. To classify the patient's retinopathy complexity, the features from both inputs are transferred into the classifier with the diabetes dataset. Figure 1 depicts the proposed mechanism's block diagram.

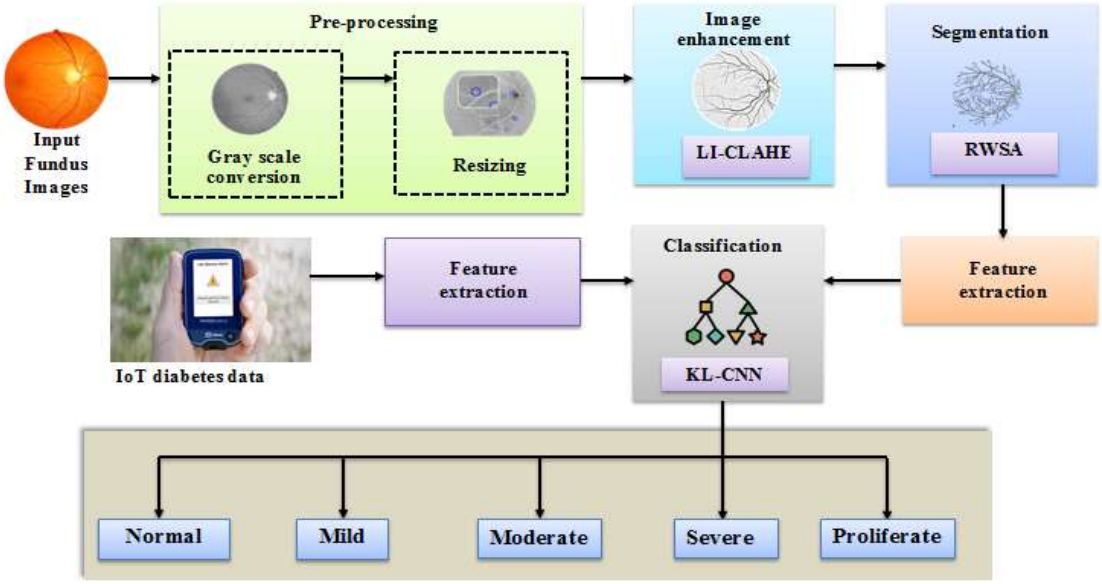

Figure 1: Block Diagram of the Proposed Methodology

3.1. Retina image

In this phase, the processing stages of the proposed system by utilizing a retina fundus image are explicated. Before classification, the observed input image is handled for some crucial steps as follows.

3.1.1. Preprocessing

Since pre-processing elevates the performance of the system, it is the prominent step of any medical image. As per this state, this proposed paper carries two steps of preprocessing.

(a) Conversion to grayscale

For facilitating the blood vessels segmentation and decreasing the computational time, the Color fundus image (I) is initially transformed into a gray-scale image, which offers only the luminance information as of the color image after eliminating the hue and saturation. The conversion is expressed as, (Ghoshal, R., Saha, A., & Das, S. (2019))

$$G = \left(0.2989\mathrm{R} + 0.5870\mathrm{G} + 0.1140\mathrm{B}\right) \in I \tag{1}$$

Where, the fundus image's red, green, and blue color is indicated as R, G and B, correspondingly.

(b) Resizing

To have the same radius, the gray images are resized. Also, it is cropped for avoiding uninformative black pixels around the edges. The preprocessed image is signified as F_n^{pre} .

3.1.2. Image enhancement

By utilizing the LI-CLAHE algorithm, valleys and ridges of the preprocessed Image F_n^{pre} are enhanced. The prevailing CLAHE is applied over all neighborhood pixels for enhancing the image's contrast. However, the prevailing approach has the limitations of the disappearance of vascular lines and edges while removing the artificial boundary tiles. To draw an eradicated line within the range of a discrete set of previously identified data points, linear interpolation assists in constructing new data points. Also, it efficiently recognized the disappeared minute line by estimating the linear relationship between the known data points. So, long disappeared lines can also be computed easily. Thus, for assessing vanished edges as of the given input image's vector, the simplest methodology is a Linear interpolation. Thus, the proposed paper uses linear interpolation rather than bilinear interpolation. Preprocessed image is partitioned into contextual regions. Then, a histogram of the contextual regions is calculated. After that, the number of pixels (m_g) is equally divided for every single GL in the histogram. So, the average number of pixels in the GL $P_{avg} \in F_n^{pre}$ is computed as, (Kumar, S., & Kumar, B. (2018))

$$P_{avg} = \frac{m_k * m_j}{m_g} \tag{2}$$

Where, the contextual region's number of pixels in the x direction and y direction is denoted as m_k and m_j, correspondingly. The actual clip limit $F_{(n)CL}$ is expressed as,

$$F_{(n)CL} = P_{avg} * C_l \tag{3}$$

Where, C_l signifies the number of clip levels. The pixels can be redistributed for each GL utilizing the threshold limit. After performing the equalization, the neighboring tiles are combined utilizing linear interpolation (F_n^{enhan}) . The linear interpolation is derived by pondering '2' known points. It is calculated as,

$$F_n^{enhan} = \left(v_{(1)tile} + \frac{(u_{ima} - u_{(1)tile})(v_{(2)tile} - v_{(1)tile})}{u_{(2)tile} - u_{(1)tile}} \right) \in F_{(n)CL} \tag{4}$$

Where, u_{ima} is the point of an input image, $u_{(1)tile}$ and $v_{(1)tile}$ are the first coordinates of the tile, $u_{(2)tile}$ and $v_{(2)tile}$ are the second coordinates of the tile.

3.1.3. Segmentation

The enhanced image is given in the RWSA. The watershed segmentation system is grounded on the concept of image intensity's topographic representation. The blood vessel is partitioned by the watershed lines via the topographic representation process. However, the prevailing segmentation is highly sensitive to local

minima since the leakage occurs. The leakage moves towards the unwanted parts, which makes an image over-segmentation. To avoid this, the similarity score for the nearest pixel is computed to make the appropriate segmentation.
Primarily, for separating the pixels into foreground and background areas, the thresholding function is applied. The output of this process gives the binary image as,

$$F_n^{enhan} \xrightarrow{Conversion} \left(F_n^{enhan}\right)_{bin} \tag{5}$$

Where, $\left(F_n^{enhan}\right)_{bin}$ represents a binary image with white and black pixels. After that, for creating watershed lines betwixt two regions, the similarity (S) between every pixel is measured utilizing the RESNIK. It is derived by the maximal likelihood betwixt the white and black pixels. The similarity score can be articulated as,

$$S = \max\left[-\chi \in \left(F_n^{enhan}\right)_{bin}\right] \tag{6}$$

Wherein, χ signifies the likelihood betwixt the white and black pixels. From the similarity function, the coordinates of the local maxima, which are known as foreground markers, are extracted for finding the catchment basins. After that, the watershed function is implemented for segmentation as,

$$F_{(n)seg}^{enhan} = W(\vartheta \cap (R_i)) \tag{7}$$

Where, the set of local maxima points closer to the other regional minimum R_i is represented as $\vartheta \in S$, and the watershed function that updates the markers grounded on the labels is indicated as W. Thus, the binary image is attained with the partitioned regions utilizing watershed lines. The water body area is automatically segmented by the watershed function from the image.

3.1.4. Feature extraction

One of the major roles is played by Feature extraction, which aids in identifying the status of the blood vessels. Thus, the key vesselness features, namely HARALICK, ADTCWT, centerline, circularity index, the maximum and minimum diameter of the vessel, entropy, vascular length, branches of vessels, and vascular density are extracted from the segmented blood vessels. The features also expose the retina's status. The necessary features are expressed as,

$$f_n = \{f_1, f_2, f_3, \ldots\ldots f_N\} \tag{8}$$

Wherein, f_n epitomizes the number of extracted features.

3.2. IoT diabetes data

The diabetes data, which has the relevant diabetes details of the input fundus image, is considered as another input of the proposed system. It has been observed from the patient's body utilizing an IoT-based Glucometer. The device has a dimension of 3.6 in x 2.3 in x 0.9 with a weight of 0.2 lbs. (75 g) along with the storage of 400 glucose measurements. The data carries attributes of glucose, insulin, diabetes pedigree function, blood pressure, body mass index, along with age. The complexity of retinopathy is classified in the classification step grounded on ranges represented under the attributes. The attributes (E_n) presented in the diabetic dataset are initialized as,

$$E_n = \{E_1, E_2, E_3, ...E_N\} \tag{9}$$

3.3. Classification

The features attained from the two phases are directly given into the KL-CNN. CNN, which is designed to automatically learn features, is a type of DL model for processing data. Numerous classifications are present from which CNN is recommended for its specific characteristics of managing a huge number of parameters. However, the conventional CNN may lose more features when features are extracted by the pooling operation. Thus, the kriging layer is wielded instead of a pooling layer. It selected minimum spatial features without losing the meaning. Figure 2 elucidates the proposed KL-CNN's architecture,

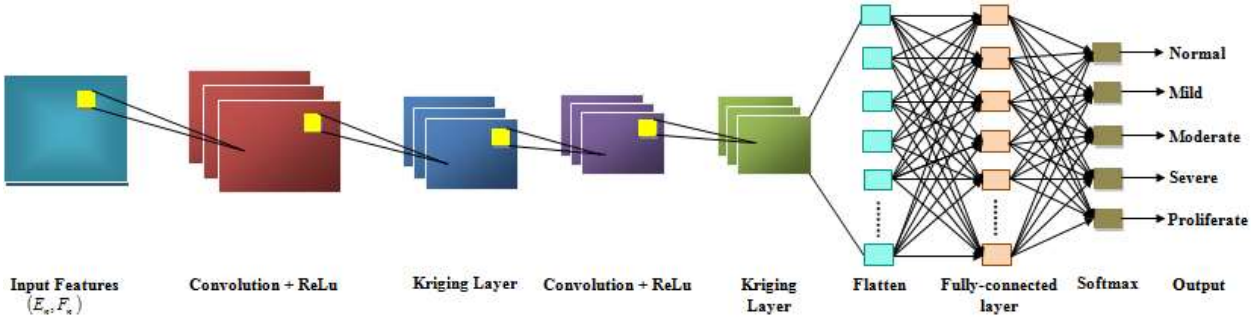

Figure 2: Architecture of the Proposed KL-CNN

Initially, the input features are directly given into the convolution layer, which extracts the features by applying an element-wise product betwixt the kernel's every single element and the input array. It could be expressed as,

$$\varphi = \sum_d \sum_d ((f_n)(E_n))(r-d, s-d) * \omega(d,d) \tag{10}$$

Where, φ and $\omega(d,d)$ epitomize the output of the convolution operation and kernel in the dimension size $d \times d$, r and s are the dimension size of the input matrix. Following this, nonlinearity is used to cut off the generated features based on the ReLU activation function $(\hbar)$, which is expressed as, **(**Kwasigroch, A., Jarzembinski, B., & Grochowski, M. (2018))

$$\hbar = \max(0, \varphi) \tag{11}$$

By attaining a kriging layer (K), the extracted features are further reduced. It converts the features by implementing the dot product betwixt the convoluted features and input features. It is expressed as,

$$K = \sum_{i=1}^{N} \varphi\omega(f_n, E_n) \tag{12}$$

Kriging states the statistical surface as a regionalized variable, with a certain degree of continuity. The Kriging estimate is known as the Best Linear Unbiased Estimate (BLUE), because it is a linear combination of the weighted features, whose expected value for error equals zero and whose variance is a minimum. It provides the appropriate information without losing the originality of features. The aforementioned two processes are continued till they reach the fully connected layer. A fully connected layer is flattened into a one-dimensional array of numbers. After that, the flattened output is computed as,

$$\xi = K - \left(\omega\left(d \times d\right) - 1\right) \tag{13}$$

Where, ξ is the fully connected layer's output. The CNN is familiar with the softmax activation function $\left(\wp\right)$ to normalize output real values in the range of $\left[0,1\right]$. It is given as,

$$\wp = \frac{e^{\xi_i}}{\sum_{i=1}^{N} \xi_i} \tag{14}$$

Where, ξ_i symbolizes the fully connected layer output at the ith node and the total number of output nodes are indicated as N. After training the model, testing is performed, and classified its classes as normal, mild, moderate, severe, and proliferates. Lastly, the loss function L is calculated as,

$$L = T - \wp \tag{15}$$

Wherein, T epitomizes the targeted class. The pseudo-code of the proposed KL-CNN is,

---

Input: extracted features $E_n f_n$

Output: classification of complexities $\wp$

Begin

Initialize parameters $\aleph_n, \hbar$, maximum Iteration $It_{\max}$

Initialize weight value

Set $It = 1$

While $\left(It \le It_{\max}\right)$

Compute convolution operation φ

Evaluate activation function

$$\hbar = \max\left(0, \varphi\right)$$

Reduce feature map by kriging layer

Flattening all the layers

Activate neurons by $\wp = \frac{e^{\xi_i}}{\sum_{i=1}^{N} \xi_i}$

If $\left(loss == t\arg et\right)$ {

Terminate

} **Else** {

$It = It + 1$

}

End If

End While

Return classified output

End

After attaining the desired classes, the performance of every novelty is analyzed with some quality metrics in the following results section.

4. RESULTS AND DISCUSSION

The proposed DR detection model's performance is experimentally evaluated in comparison with the conventional approaches. In the working platform of MATLAB, the proposed model is employed. For experimental analysis, the data is synthetically designed by gathering data from a publicly available resource. From this, 60% of the dataset is utilized for training, 20% is employed for testing and 20% is utilized for validation.

4.1. Hardware requirements

The proposed approach is employed in the working platform of MATLAB/SIMULINK (version R2020a) with machine configuration as follows:

- Processor: Intel core i3
- CPU Speed: 2.20 GHz
- OS: Windows 7
- RAM: 4GB

4.2. Software requirements

In the working platform of MATLAB, the proposed model will be implemented. A multi-paradigm numerical calculating environment with a fourth-generation programming language is named MATLAB (matrix laboratory). Specifically for quick as well as easy scientific calculations and I/O, this is designed. MathWorks developed a proprietary programming language. MATLAB permits matrix manipulations, plotting of functions and data, algorithm implementation, generation of user interfaces, as well as interfacing with programs written in other languages, incorporating C, C++, C#, Java, Fortran, along with Python.

4.3. Performance analysis of image enhancement

With the prevailing approaches like CLAHE, Histogram Equalization (HE), and Contrast Stretching (CS), the proposed LI-CLAHE's performance is evaluated and analogized.

The performance analysis of the proposed and prevailing mechanisms is depicted in figure 3. For measuring the image's quality, PSNR is wielded. A higher PSNR value gives better quality to the proposed model. Better quality to the proposed system is given by the higher PSNR value. The proposed one attains a PSNR of 33.25 db, whereas the PSNR of the prevailing models is 29 db for CLAHE and 24.426 db for HE. The cumulative squared error betwixt the compressed and the original image was represented by MSE. The MSE of the proposed model is 122, which is lower than the prevailing approaches. The image quality degradation caused by processing like data compression is quantified by a perceptual metric named SSIM. Similarly, the SSIM attained by the proposed technique is 0.9989. Therefore, it is proved that the proposed framework is efficient for all metrics.

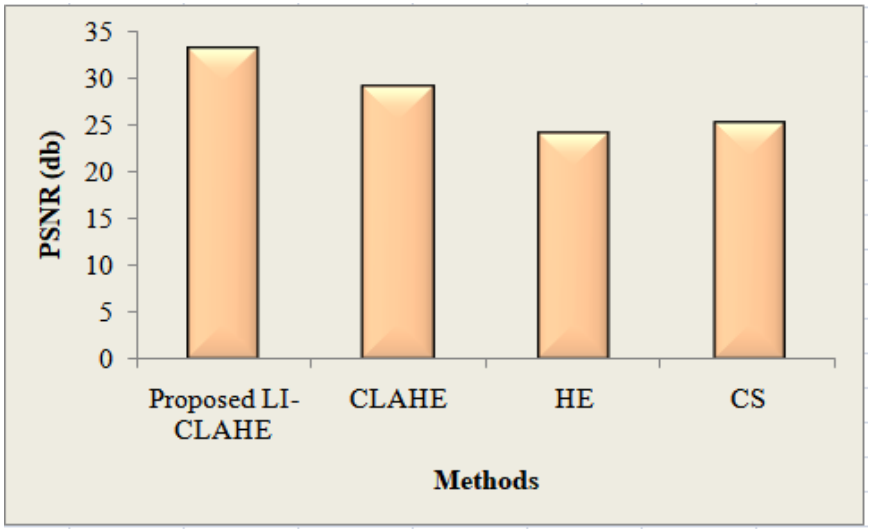

(a)

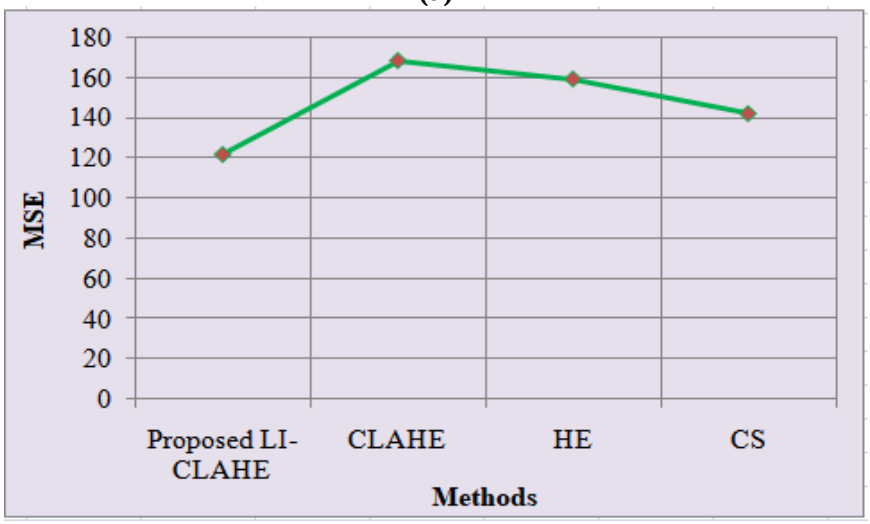

(b)

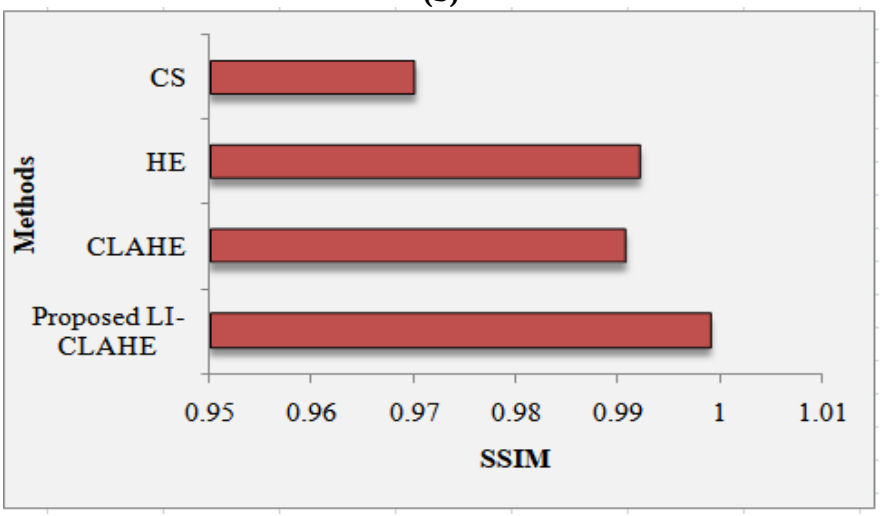

(c)

Figure 3: Performance Analysis of Proposed Model and Existing Model, (a) Peak Signal to Noise Ratio (PSNR), (b) Mean Square Error (MSE), (c) Structural Similarity Index (SSIM)

4.4. Performance analysis of segmentation

With the prevailing K-Means (KM), Region Growing (RG), Active Contour (AC), along with Fuzzy C-Means (FCM), the proposed RWSA's performance is analogized regarding several quality metrics.

Table 1: Performance Analysis of Proposed RWSA and Existing Models

(a)

Techniques/Metrics	Sensitivity	Specificity	Accuracy	Precision
Proposed RWSA	97.2327	94.8744	97.9882	94.1661
AC	94.0018	89.2256	94.1005	90.3586
KM	92.4932	87.8355	89.1132	87.4312
FCM	88.3574	84.4725	87.9224	85.2644
RG	84.7232	81.8451	82.1482	80.9511

(b)

Techniques/Metrics	Recall	f-measure	NPV	MCC
Proposed RWSA	96.2327	91.74527	96.19128	94.9563
AC	93.0018	89.28475	93.17838	91.9839
KM	90.4932	86.21732	89.21422	90.0335
FCM	89.3574	83.84717	88.98433	88.2068
RG	84.7232	83.33212	84.33341	86.7747

The comparative assessment of the proposed and prevailing techniques is illustrated in table 1. The proposed technique's higher performance is represented by the aforementioned metrics' higher value. Sensitivity measures the percentage of actual positive value, which is identified correctly. Similarly, specificity gauges the percentage of actual negative value, which is correctly identified. The sensitivity displayed an enhancement of 3% more than AC. Likewise, the specificity of the proposed model attains an improvement of 7.0389% than KM. The accuracy of the proposed model is analyzed and shows its improvement by 3.8877%, a precision of 3.8075% higher than AC, f-measure of 7.8981% higher than FCM. The Negative Predictive Value (NPV) of the proposed method shows an improvement of 11.857% more than RG and Matthew's correlation coefficient (MCC) of 2.9724% more than AC. These result enhancements can be attained only by focusing more interest on the unimproved segments. From the overall analysis, it is concluded that the proposed technique displays efficient performance when contrasted with the prevailing approaches.

4.5. Performance analysis of classification

The proposed KL-CNN is analogized with the prevailing techniques like CNN, DNN, ANN, along with RNN for proving the developed model's superiority.

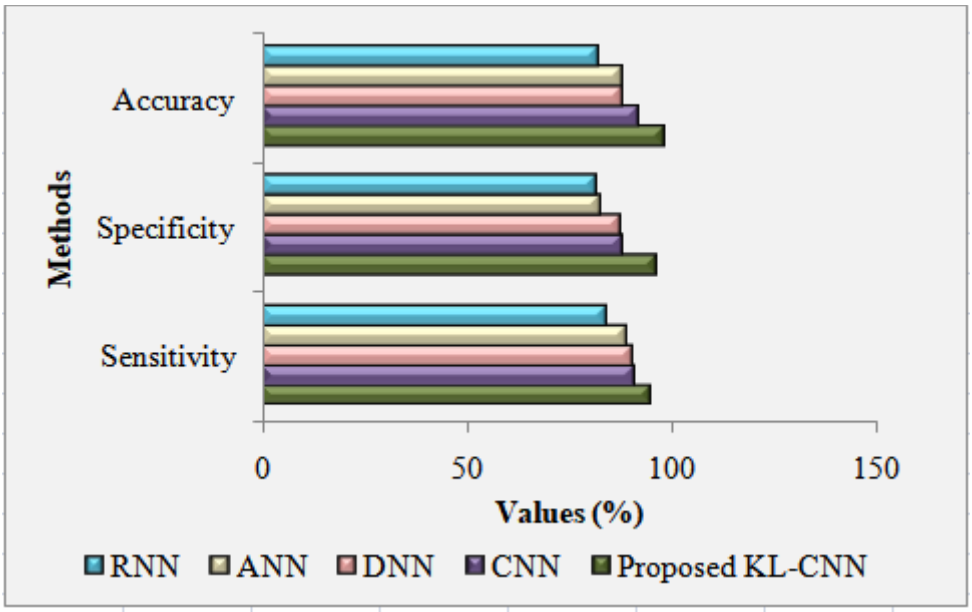

(a)

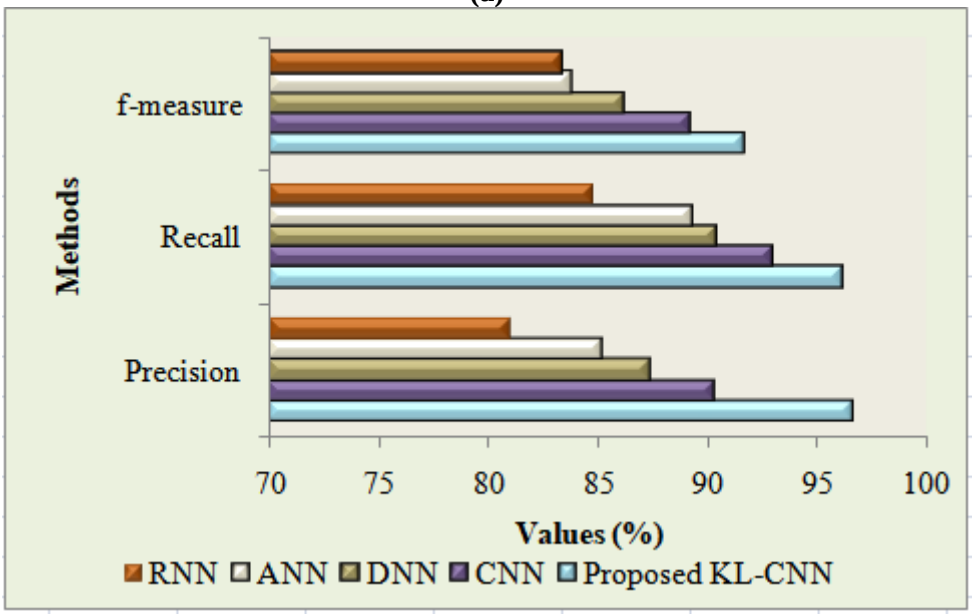

(b)

Figure 4: Performance Analysis of the Proposed KL-CNN and the Existing Models in terms of (a) Sensitivity, Specificity, and Accuracy, (b) Precision, Recall, and F-Measure

Figure 4 displays the performance evaluation of the proposed KL-CNN and the conventional frameworks. The proposed model attains a sensitivity of 95.33%, which is higher than the prevailing models, which attain sensitivity in the range of 87% to 93%. Likewise, higher specificity, accuracy, and precision values show the proposed model's superior performance. The proposed model attains a specificity of 96.4%, an accuracy of 98.4%, a precision of 96.7%, a recall of 96.23%, and an f-measure of 91.7%, which are superior to the conventional techniques.

Table 2: Performance Analysis of Proposed KL-CNN and Existing Models

Techniques/ Metrics	FPR (%)	FNR (%)	FRR (%)
Proposed KL-CNN	3.55	1.40	1.40
CNN	29.10	48.24	48.24
DNN	48.38	44.43	44.43
ANN	51.36	61.55	61.55
RNN	66.87	81.01	81.01

Regarding the False Rejection Rate (FRR), False Negative Rate (FNR), together with False Positive Rate (FPR), the performance analysis of the proposed KL-CNN and prevailing methodologies is shown in table 5. The models' better performance is indicated by the lower values of FPR, FNR, and FRR. The FPR of the proposed model shows an improvement of 25.55% than the existing CNN and 44.83% more than DNN. Likewise, the FNR and FRR of the proposed model are the same, which are also lesser than the existing models and show an improvement of 46.84% than CNN, 43.03% than DNN, 62.15% than ANN, and 78.61% than RNN. The higher results can be reached by replacing the kriging layer, which reduces the features for improving training time whereas the reduced features can be obtained without losing the information. Also, the best results can be obtained in the DR detection system with the consideration of efficient data from IoT sensor data. From these, it is proved that the proposed KL-CNN shows better performance for the classification of complexities.

4.6. Performance analysis based on objectives

The proposed KL-CNN's performance is analogized with CNN, SVM, and DNN.

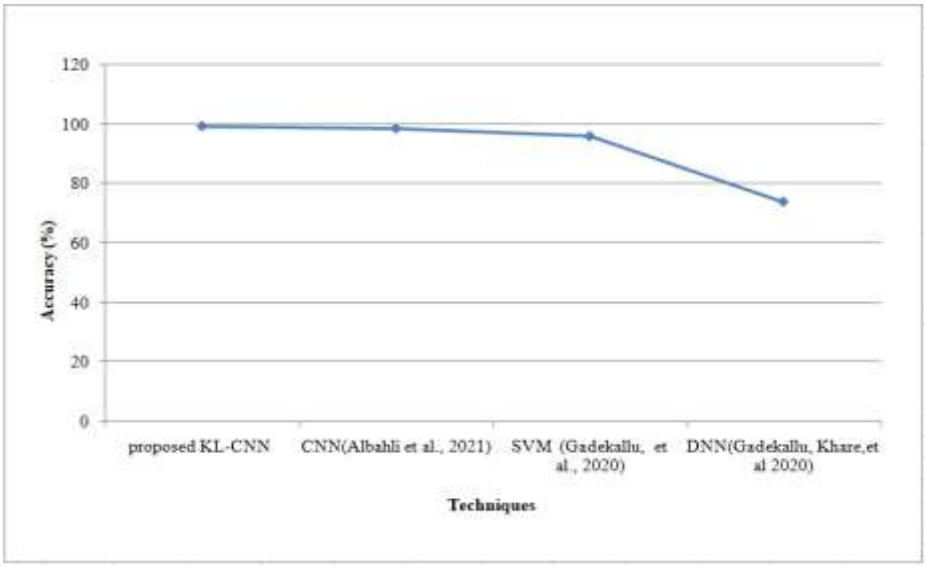

Figure 5: Comparative Analysis of the Proposed Method with the Existing Method

Regarding accuracy, the proposed system's performance with the conventional frameworks is elucidated in figure 5. The proposed work considers the IoT details and accurate segmentation of blood vessels. By this accurate processing, the proposed approach could attain superior outcomes when analogized with the prevailing systems, that is, 99.4%. In existing, they are not considering IoT sensor data with the retina image. This is one of the reasons to obtain better results in the classification. Therefore, it is shown that the proposed technique outperforms the prevailing algorithms.

5. CONCLUSION

This work proposes a novel KL-CNN classifier for DR detection. The proposed technique undergoes preprocessing, image enhancement, segmentation, feature extraction, and classification. After executing all the steps, the experimental evaluation is performed on the performance of the proposed KL-CNN and RWSA. Also, it was assessed and analogized with the prevailing techniques. The final outcomes unveil that the proposed model attains an accuracy of 98.4%. Likewise, the proposed technique attains the best outcome for all other metrics, such as sensitivity, specificity, precision, recall, f-measure, NPV, MCC, FPR, FNR, and FRR. Thus, from the overall analysis, it is determined that the proposed technique is highly efficient for the classification of complexities when contrasted with the prevailing systems. The work is developed by considering very few amounts of features. By considering features on each layer of the retina image, the work will be extended for the advanced detection of retinopathy in the future.

REFERENCES

Albahli, S., Nazir, T., Irtaza, A., & Javed, A. (2021). Recognition and detection of diabetic retinopathy using densenet-65 based faster-rcnn. *Computers, Materials and Continua*, *67*(2), 1333–1351. https://doi.org/10.32604/cmc.2021.014691

Bibi, I., Mir, J., & Raja, G. (2020). Automated detection of diabetic retinopathy in fundus images using fused features. *Physical and Engineering Sciences in Medicine*, *43*(4), 1253–1264. https://doi.org/10.1007/s13246-020-00929-5

Chaudhary, S., & Ramya, H. R. (2020). Detection of diabetic retinopathy using machine learning algorithm. *2020 IEEE International Conference for Innovation in Technology, INOCON 2020*, 1–5. https://doi.org/10.1109/INOCON50539.2020.9298413

Chen, W., Yang, B., Li, J., & Wang, J. (2020). An approach to detecting diabetic retinopathy based on integrated shallow convolutional neural networks. *IEEE Access*, *8*, 178552–178562. https://doi.org/10.1109/ACCESS.2020.3027794

Gadekallu, T. R., Khare, N., Bhattacharya, S., Singh, S., Maddikunta, P. K. R., Ra, I. H., & Alazab, M. (2020). Early detection of diabetic retinopathy using pca-firefly based deep learning model. *Electronics (Switzerland)*, *9*(2), 1–16. https://doi.org/10.3390/electronics9020274

Gadekallu, T. R., Khare, N., Bhattacharya, S., Singh, S., Maddikunta, P. K. R., & Srivastava, G. (2020). Deep neural networks to predict diabetic retinopathy. *Journal of Ambient Intelligence and Humanized Computing*, *0123456789*. https://doi.org/10.1007/s12652-020-01963-7

Habib Raj, M. A., Mamun, M. Al, & Faruk, M. F. (2020). CNN Based diabetic retinopathy status prediction using fundus images. *2020 IEEE Region 10 Symposium, TENSYMP 2020*, *June*, 190–193. https://doi.org/10.1109/TENSYMP50017.2020.9230974

Jayakumari, C., Lavanya, V., & Sumesh, E. P. (2020). Automated diabetic retinopathy detection and classification using imagenet convolution neural network using fundus images. *Proceedings - International Conference on Smart Electronics and Communication, ICOSEC 2020*, *Icosec*, 577–582. https://doi.org/10.1109/ICOSEC49089.2020.9215270

Kolla, M., & Venugopal, T. (2021). Efficient Classification of diabetic retinopathy using binary CNN. *Proceedings of 2nd IEEE International Conference on Computational Intelligence and Knowledge Economy, ICCIKE 2021*, 244–247. https://doi.org/10.1109/ICCIKE51210.2021.9410719

Li, Q., Peng, C., Ma, Y., Du, S., Guo, B., & Li, Y. (2021). Pixel-level diabetic retinopathy lesion detection using multi-scale convolutional neural network. *LifeTech 2021 - 2021 IEEE 3rd Global Conference on Life Sciences and Technologies*, *LifeTech*, 438–440. https://doi.org/10.1109/LifeTech52111.2021.9391891

Maneerat, N., Thongpasri, T., Narkthewan, A., & Kimpan, C. (2020). Detection of hard exudate for diabetic retinopathy using unsupervised classification method. *Proceedings - 2020 6th International Conference on Engineering, Applied Sciences and Technology, ICEAST 2020*, *i*, 5–8. https://doi.org/10.1109/ICEAST50382.2020.9165498

Mateen, M., Wen, J., Nasrullah, N., Sun, S., & Hayat, S. (2020). Exudate detection for diabetic retinopathy using pretrained convolutional neural networks. *Complexity*, *2020*. https://doi.org/10.1155/2020/5801870

Math, L., & Fatima, R. (2021). Adaptive machine learning classification for diabetic retinopathy. *Multimedia Tools and Applications*, *80*(4), 5173–5186. https://doi.org/10.1007/s11042-020-09793-7

Pao, S. I., Lin, H. Z., Chien, K. H., Tai, M. C., Chen, J. T., & Lin, G. M. (2020). Detection of diabetic retinopathy using bichannel convolutional neural network. *Journal of Ophthalmology*, *2020*. https://doi.org/10.1155/2020/9139713

Qiao, L., Zhu, Y., & Zhou, H. (2020). Diabetic retinopathy detection using prognosis of microaneurysm and early diagnosis system for non-proliferative diabetic retinopathy based on deep learning algorithms. *IEEE Access*, *8*, 104292–104302. https://doi.org/10.1109/ACCESS.2020.2993937

Rajkumar R.S., Ragul, D., Jagathishkumar, T., & Selvarani, A. G. (2021). Transfer learning approach for diabetic retinopathy detection using efficient network with 2 phase training. *2021 6th International Conference for Convergence in Technology, I2CT 2021*, 1189–1193. https://doi.org/10.1109/I2CT51068.2021.9418111

Sabbir, M. M. H., Sayeed, A., & Jamee, M. A. U. Z. (2020). Diabetic retinopathy detection using texture features and ensemble learning. *2020 IEEE Region 10 Symposium, TENSYMP 2020*, *June*, 178–181. https://doi.org/10.1109/TENSYMP50017.2020.9230600

Samanta, A., Saha, A., Satapathy, S. C., Fernandes, S. L., & Zhang, Y. D. (2020). Automated detection of diabetic retinopathy using convolutional neural networks on a small dataset. *Pattern Recognition Letters*, *135*, 293–298. https://doi.org/10.1016/j.patrec.2020.04.026

Trisha, & Ali, I. (2020). Intensity based optic disk detection for automatic diabetic retinopathy. *2020 International Conference for Emerging Technology, INCET 2020*, 1–5. https://doi.org/10.1109/INCET49848.2020.9154021

Tymchenko, B., Marchenko, P., & Spodarets, D. (2020). Deep learning approach to diabetic retinopathy detection. *ICPRAM 2020 - Proceedings of the 9th International Conference on Pattern Recognition Applications and Methods*, 501–509. https://doi.org/10.5220/0008970805010509.

Ghoshal, R., Saha, A., & Das, S. (2019). An improved vessel extraction scheme from retinal fundus images. *Multimedia Tools and Applications*, *78*(18), 25221–25239. https://doi.org/10.1007/s11042-019-7719-9

Kumar, S., & Kumar, B. (2018). Diabetic Retinopathy Detection by Extracting Area and Number of Microaneurysm from Colour Fundus Image. *2018 5th International Conference on Signal Processing and Integrated Networks, SPIN 2018*, 359–364. https://doi.org/10.1109/SPIN.2018.8474264

Kwasigroch, A., Jarzembinski, B., & Grochowski, M. (2018). Deep CNN based decision support system for detection and assessing the stage of diabetic retinopathy. *2018 International Interdisciplinary PhD Workshop, IIPhDW 2018*, 111–116. https://doi.org/10.1109/IIPHDW.2018.8388337